



## Plastic yield inception of an indented coated flat and comparison with a flattened coated sphere

Wenping Song<sup>a,b,\*</sup>, Longqiu Li<sup>a</sup>, Andrey Ovcharenko<sup>b</sup>, Ding Jia<sup>a</sup>, Izhak Etsion<sup>c</sup>, Frank E. Talke<sup>b</sup>

<sup>a</sup> School of Mechatronics Engineering, Harbin Institute of Technology, Harbin, China

<sup>b</sup> Center for Magnetic Recording Research, University of California, San Diego, CA, USA

<sup>c</sup> Department of Mechanical Engineering, Technion-Israel Institute of Technology, Haifa, Israel

### ARTICLE INFO

#### Article history:

Received 11 January 2012

Received in revised form

22 April 2012

Accepted 24 April 2012

Available online 3 May 2012

#### Keywords:

Spherical indentation

Hard coating

Yield inception

### ABSTRACT

The yield inception of a deformable hard coated half space indented by a rigid sphere is studied. The effect of coating thickness, sphere radius and material properties of both the coating and substrate on the critical contact parameters at yield inception is investigated. Dimensionless empirical expressions for the critical load, critical contact area and critical interference are derived as functions of a dimensionless hard coating parameter. Three different locations of the yield inception of the coated system are observed. A comparison is made with the case of a flattened coated sphere.

© 2012 Elsevier Ltd. All rights reserved.

### 1. Introduction

In many engineering applications, such as cutting tools, hard disk drives and electrical circuits, thin coatings have been widely used to improve the performance of mechanical components. The application of thin coatings on a substrate is also a common way to improve the tribological properties of components during multiple contacts and sliding. In particular, hard coatings, such as ceramics, DLC (diamond-like carbon) and titanium alloys are widely used as protective coatings to reduce friction and wear, see, e.g., Refs. [1–5].

A large volume of studies can be found in the literature on the indentation problem associated with coated substrates (see Fig. 1(a)). One of the main goals of these studies is the characterization of mechanical properties of the coatings by indentation tests, see, e.g., Refs. [6–12]. Analyzing the indentation of coated surfaces is much more complicated compared to the indentation of homogeneous un-coated solids, see, e.g., Ref. [13]. Semi-analytical solutions, which involve numerical procedures, are generally used to analyze the elastic indentation of coated substrates. Jaffar [14] developed a numerical method for an elastic coating/rigid substrate system indented by a punch. Ramalingam and Zheng [15] provided an analytical solution for the stresses at the coating/substrate interface for a pure elastic contact. In addition, a displacement formulation was proposed to calculate the stresses. Li and Chou [16] provided a theoretical solution of the elastic response of a coated substrate indented by

a parabolic load distribution. They found that the contact behavior was sensitive to the coating thickness and to the ratio of the elastic moduli of the coating and the substrate. In addition, a discontinuity of radial stress was observed at the interface. They also found that a substrate with a hard coating experienced lower normal stress than a homogeneous un-coated substrate. Schwarzer [17] developed a mathematical method to calculate the stress field and displacement of a coated substrate under any given stress distribution on the surface. Fretigny and Chateauminois [18] presented an integral transform method for calculating the elastic stress field in a coated substrate under an axisymmetric external pressure. Hsueh and Miranda [19] developed an analytical model for a Hertzian indentation of a coated substrate. A dimensionless indenter displacement, normalized with the indentation depth on an infinitely thick coating, was described as a function of the coating-thickness-to-contact-radius ratio and the coating-to-substrate Young's moduli ratio. In a related paper, Hsueh and Miranda [20] obtained an empirical solution for the coating-thickness-to-contact-radius ratio, which was combined with the previous analytical model to calculate the indenter displacement and normal load for a given contact radius of a specified coating/substrate system.

For analyzing elastic-plastic deformation of coated substrates finite element methods are commonly used. Komvopoulos [21,22] and Kral et al. [23,24] studied elastic-plastic indentation of coated surfaces. They found that the coating thickness and mechanical properties of the coating and the substrate significantly affect the contact pressure and the stress distribution in the coating and the substrate. In Ref. [22], it was found that for a ceramic coating on a metallic substrate the onset of plastic deformation always occurs at the coating/substrate interface. Sen et al. [25] studied an

\* Corresponding author.

E-mail address: [wenping.song1985@gmail.com](mailto:wenping.song1985@gmail.com) (W. Song).

### Nomenclature

$P$	load.
$A$	contact area.
$\omega$	interference.
$a$	contact radius.
$t$	coating thickness.
$R$	radius of sphere.
$E$	Young's modulus.
$Y$	yield strength.
$\nu$	Poisson's ratio.
$\kappa'$	modified critical interference ratio, $(\omega_{c\_co}/\omega_{c\_su})(E_{co}/E_{su})$ .
$\lambda_h$	hard coating parameter.
$p$	contact pressure.

$A'$	truncated contact area.
$a'$	truncated contact radius.
$\alpha$	geometrical parameter depending on indenter shape.

### Subscripts

$c$	critical value.
$c\_co$	critical value of a flat made of the coating material.
$c\_su$	critical value of flat made of the substrate material.
$co$	coating.
$su$	substrate.
$p$	corresponds to peak values.
$m$	mean value.
$e$	equivalent value.

indentation of an elastic sphere into a compliant substrate with a stiffer coating. Similar to that in Ref. [22] it was found that yielding always started at the coating/substrate interface, and that the stress was discontinuous at the interface due to the assumption of perfect bonding between the coating and the substrate. Djabella and Arnell [26] analyzed the elastic stresses in single, double and multilayer media combining finite element analysis and the Hertz theory. They found that the stresses in the coated substrate depend on the ratio of the coating thickness to the contact radius and the ratio of the Young's moduli of the coating and the substrate. Sun et al. [27] investigated the indentation of a rigid sphere into various TiN coating/substrate systems. The dimensionless critical load at the onset of plastic deformation,

normalized by the critical load of an un-coated substrate, was presented as a function of a normalized coating thickness  $t/R$  in the range of  $0 \leq t/R \leq 0.09$ , where  $t$  is the coating thickness and  $R$  is the radius of the sphere. A loading bearing capacity, in which the dimensionless critical load first decreases with the coating thickness when the coating is very thin and then increases with the coating thickness when the coating is thick, was predicted. They also found that a very thin hard coating would weaken the coated substrate. Hu and Lawn [28] developed a formulation to predict the indentation stress as a function of the indentation strain  $a/R$  in a coated substrate, where  $a$  is the contact radius and  $R$  is the radius of the spherical indenter. Wang et al. [29] evaluated the effect of substrate on the mechanical response of a coated substrate indented by a rigid conical indenter. A "substrate factor" was obtained related to the load–displacement curve, which can be fitted as a power function. All the above investigations [21–29] concerned a certain specific combination of materials for the coated system and did not present a general solution.

It was shown in several studies of elastic–plastic spherical contact that a universal dimensionless model can be obtained by normalizing the contact parameters with respect to their corresponding critical values at yield inception, see, e.g., Refs. [30,31]. The critical contact parameters for flattened solid sphere (see Ref. [32]) and flattened spherical shell (see Refs. [33,34]) under both slip and stick contact conditions were presented. More recently Goltsberg et al. [35] studied the yield inception of a flattened coated sphere and presented the critical contact parameters for a specific case of  $E_{su}/Y_{su}=952$ , where  $E_{su}$  and  $Y_{su}$  are the Young's modulus and Yield strength of the spherical substrate, respectively.

A comparison of flattening and indentation of spherical elastic–plastic contact for homogenous un-coated surfaces is presented in Ref. [31]. However, no similar comparison could be found in the published literature for a coated spherical contact. To fill this gap, the present work first explores a dimensionless solution for yield inception of an indented coated half space. Critical contact parameters are then presented for a wide range of material properties. Finally, the results for an indented coated half space are compared with the results for a flattened coated sphere presented in Ref. [35].

## 2. Modeling

### 2.1. Background

The classical Hertz theory, see, e.g., Ref. [13], provides a solution for the case of a rigid sphere with a radius  $R$  indenting an elastic half space. The relations between the normal load  $P$ , the

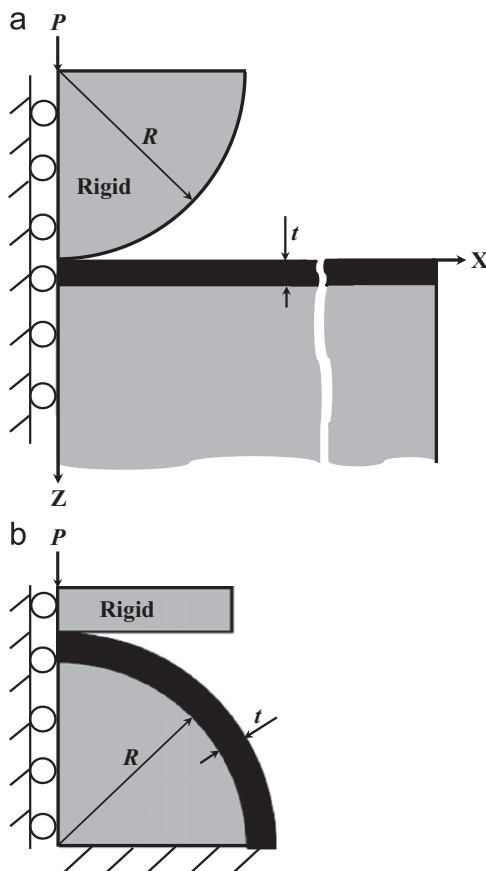


Fig. 1. Schematic of a coated spherical contact: (a) indentation and (b) flattening.

interference  $\omega$  and the contact radius  $a$ , for frictionless contact condition, are given by:

$$P = \frac{4ER^{1/2}\omega^{3/2}}{3(1-\nu^2)} \quad (1)$$

$$a = \sqrt{\omega R} \quad (2)$$

where  $E$  and  $\nu$  are the Young's modulus and Poisson's ratio of the half space material, respectively. The above expressions also hold for the case of an elastic sphere loaded by a rigid flat, in which case  $E$  and  $\nu$  are the corresponding material properties of the sphere.

The critical load  $P_c$  and the critical interference  $\omega_c$  at yield inception (see, e.g., Ref. [32]) are:

$$P_c = \frac{\pi^3}{6} C_v^3 Y \left( R(1-\nu^2) \frac{Y}{E} \right)^2 \quad (3)$$

$$\omega_c = \left[ C_v \frac{\pi(1-\nu^2)}{2} \left( \frac{Y}{E} \right) \right]^2 R \quad (4)$$

where  $C_v = 1.234 + 1.256\nu$ ,  $E$ ,  $Y$  and  $\nu$  are the Young's modulus, yield strength and Poisson's ratio of the sphere, respectively.

Recently, Goltsberg et al. [35] developed a model for the onset of plastic yield in a coated sphere compressed by a rigid flat as shown in Fig. 1(b) and a specific case of  $E_{su}/Y_{su} = 952$  was investigated in detail. They identified three dimensionless parameters that control the problem. These parameters are: (a) critical loads ratio  $P_{c,co}/P_{c,su}$ , (b) modified critical interferences ratio  $\kappa' = (\omega_{c,co}/\omega_{c,su})/(E_{co}/E_{su})$  and (c) coating parameter for the case of  $E_{su}/Y_{su} = 952$  given by:

$$\lambda' = \left( \frac{t}{R} \right) \left( \frac{P_{c,co}}{P_{c,su}} \right)^{-0.507} \quad (5a)$$

The subscripts "co" and "su" above correspond to the coating and substrate materials, respectively. The subscripts "c-su" or "c-co" correspond to the critical values of a solid sphere made of the substrate material or coating material, respectively.

Fig. 2(a) (obtained from Ref. [35]) presents typical results for the dimensionless critical load of the flattened coated sphere  $P_c/P_{c,co}$  at various critical loads ratios vs. the dimensionless coating thickness  $t/R$ , assuming that  $E_{su}/Y_{su} = 952$ . In Ref. [35], a peak value  $(P_c/P_{c,co})_{max}$  is observed at a certain dimensionless coating thickness  $t/R = (t/R)_p$  that was given by:

$$\left( \frac{t}{R} \right)_p = 2.838 \times 10^{-3} \left( \frac{P_{c,co}}{P_{c,su}} \right)^{0.507} \quad (5b)$$

Fig. 2(b) presents the same results of Fig. 2(a) but consolidated into a single curve by plotting them as a function of the coating parameter for the case of  $E_{su}/Y_{su} = 952$ . Empirical expressions for the dimensionless critical contact parameters are presented in Ref. [35] for the range of  $2 \leq P_{c,co}/P_{c,su} \leq 9$  and two typical values of  $\kappa'$ , i.e.,  $\kappa' = 0.678$  and  $0.31$ . They also found that the yield inception of a flattened coated sphere is dependent on  $E_{su}/Y_{su}$ . Considering the effect of  $E_{su}/Y_{su}$ ,  $(t/R)_p$  is given as

$$\left( \frac{t}{R} \right)_p = 2.824 \cdot \left( \frac{E_{su}}{Y_{su}} \right)^{-1.014} \left( \frac{P_{c,co}}{P_{c,su}} \right)^{0.536} \quad (6)$$

### 2.2. Finite element model

Fig. 3(a) presents a 2D axisymmetric finite element model of a coated half space indented by a rigid sphere. The Young's modulus of the sphere was chosen to be  $E_{sphere} = 1000E_{co}$  to model a "perfectly rigid" body.

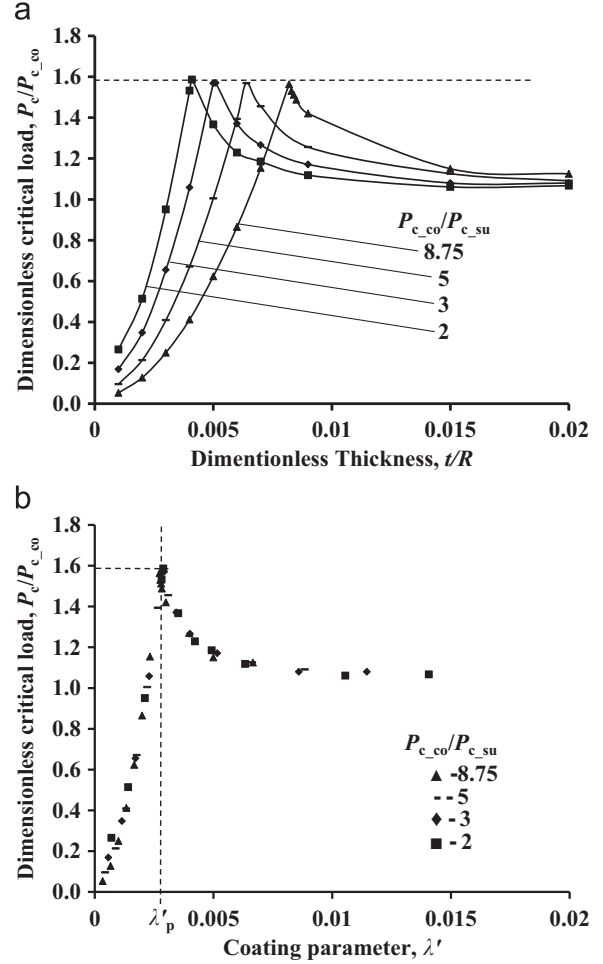


Fig. 2. Dimensionless critical load  $P_c/P_{c,co}$  of the flattened coated sphere as a function of (a) dimensionless coating thickness  $t/R$  and (b) coating parameter  $\lambda'$  for different values of critical loads ratio (presented in Ref. [35]).

The simulation was performed using an implicit integration solver with a commercially available finite element software ANSYS (version 11.0). The dimensions of the substrate were chosen to be  $4R \times 5R$  in the  $x$  and  $z$  directions, respectively.

As shown in Fig. 3(b), the coated substrate was divided into three different mesh density zones. Zone I, with a distance of  $0.015R$  from the symmetrical axis  $Z$ , contained the entire contact area as well as the zone where yield inception occurred. Zone I had the finest mesh and the typical length in  $x$  direction of the element was kept  $(1-1.5) \times 10^{-4}R$  to capture accurately the contact radius  $a$ . In this study, we assume that  $p(r) > 0$  if  $r < a$ ; otherwise,  $p(r) = 0$  if  $r \geq a$ , where  $p$  is the contact pressure and  $r$  is the distance from contact center. The contact area  $A$  was calculated by  $A = \pi a^2$ . The subzones II and III, outside the contact zone, had a gradually coarser mesh with increasing distance from the contact zone.

An eight-node quadrilateral element (PLANE 183) was used for both the sphere and the coated substrate. A three-node contact element (Conta172) and target element (Targe169) were used for the contact surfaces of the sphere and the coating, respectively. The entire model consists of 16,976–20,006 elements and 51,887–60,599 nodes depending on the dimensionless coating thickness  $t/R$ . The following boundary conditions were imposed (see Fig. 1(a) and 3(a)):

- The nodes on the axis of symmetry  $Z$  of the sphere and the coated substrate were constrained in the  $X$  direction.
- The nodes at the base of the substrate were constrained in both  $X$  and  $Z$  directions.

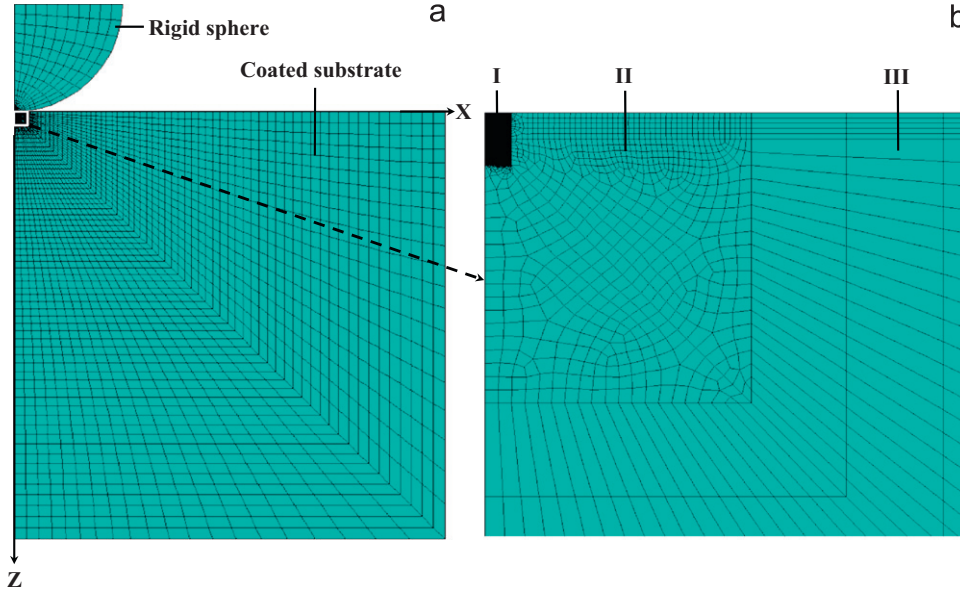


Fig. 3. Different mesh density zones (a) entire mesh and (b) zoom in of the contact region in the coated substrate.

The same assumptions defined in Ref. [35] are adopted in this study. They are: frictionless contact between the sphere and the coating, perfect bonding at the interface between the substrate and the coating, homogenous coating material and no residual stresses. A displacement control (similar to that described in Ref. [33]) was used to indent the sphere into the coated system. The von Mises yield criterion was used to detect yield inception.

The materials of both the coating and the substrate were assumed to be elastic-plastic with linear isotropic hardening of 2%. However, as was found in Ref. [30], the effect of strain hardening on the contact parameters under perfect slip contact condition is negligible for a tangent modulus less than  $0.05E$ , which is typical for most materials. Hence, the results in this paper are applicable for most materials.

The numerical model was first verified by using the same material for the coating and the substrate and comparing the results with the analytical Hertz solution. The errors in the contact load and contact area were less than 2.5%. Proper convergence of the numerical solution for the coated system was tested by refining the mesh size (increasing the number of elements) until further refinement has negligible effect. The calculation time varied from 8–20 min depending on the dimensionless coating thickness  $t/R$  using a HP workstation computer with four CPU 2.80 GHz and 8 Gb RAM.

### 3. Results and discussion

The following typical input parameters were used in the numerical simulations: the radius of the rigid sphere is  $R=10\ \mu\text{m}$ ; the dimensionless coating thickness  $t/R$  varied in the range of  $0.001 \leq t/R \leq 0.06$ . The material properties of the substrate were: Young's modulus  $E_{su}=205\ \text{GPa}$ ; yield strength  $Y_{su}$  varied in the range of  $137 \leq Y_{su} \leq 427\ \text{MPa}$  and Poisson's ratio  $\nu_{su}=0.30$ . The material properties of the coating were: Young's modulus  $E_{co}$  was varied in the range of  $223 \leq E_{co} \leq 882\ \text{GPa}$ ; yield strength  $Y_{co}$  varied in the range of  $411 \leq Y_{co} \leq 1710\ \text{MPa}$  and Poisson's ratio  $\nu_{co}=0.30$ . This was done to cover a wide range of critical loads ratio  $3.78 \leq P_{c,co}/P_{c,su} \leq 21.43$ , modified critical interferences ratio  $0.31 \leq k' \leq 2.005$  and  $480 \leq E_{su}/Y_{su} \leq 1500$ . In this study, we assumed that  $E_{co}/E_{su} > 1$ ,  $Y_{co}/Y_{su} > 1$  and  $P_{c,co}/P_{c,su} > 1$  to model a hard coating on a soft substrate.

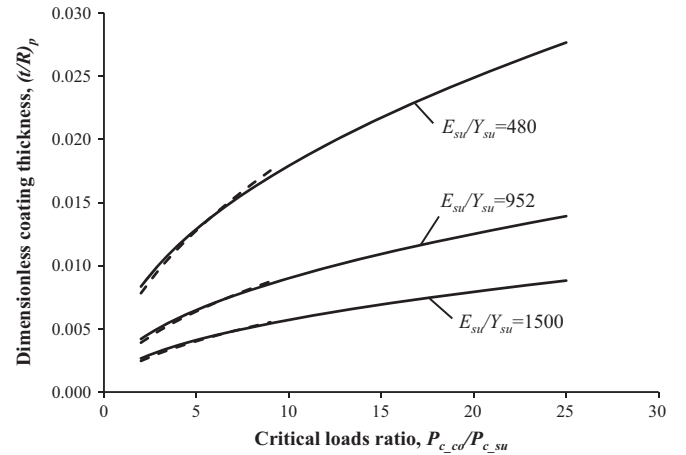


Fig. 4. Dimensionless thickness  $(t/R)_p$  versus critical loads ratio for indentation (solid lines) and flattening (dashed lines) at different values of  $E_{su}/Y_{su}$ .

A change in the sphere radius and the Young's modulus of the substrate in the range  $5 \leq R \leq 200\ \mu\text{m}$  and  $80 \leq E_{su} \leq 550\ \text{GPa}$ , respectively, had negligible effects on the dimensionless critical contact parameters,  $P_c/P_{c,co}$ ,  $\omega_c/\omega_{c,co}$  and  $A_c/A_{c,co}$ , which remain fixed as long as  $t/R$ ,  $E_{su}/Y_{su}$ ,  $P_{c,co}/P_{c,su}$ ,  $k'$  and Poisson's ratios of both the coating and the substrate were maintained constant.

Similar to the coated flattening sphere case, which was described in Ref. [35], a peak value of the dimensionless critical load  $P_c/P_{c,co}$  was also observed for the present case of indented coated half space at a certain value of  $t/R=(t/R)_p$ . By curve fitting the numerical results for  $(t/R)_p$  and the corresponding  $(P_c/P_{c,co})_{\text{max}}$ , the following expressions were obtained:

$$\left(\frac{t}{R}\right)_p = 2.94 \cdot \left(\frac{E_{su}}{Y_{su}}\right)^{-1.003} \left(\frac{P_{c,co}}{P_{c,su}}\right)^{0.474} \quad (7)$$

$$(P_c/P_{c,co})_{\text{max}} = 13.69 \cdot k'^{-0.0156} - 12.41 \quad (8)$$

Fig. 4 presents a comparison of the value of  $(t/R)_p$  for indentation (see Eq. (7)) and for flattening (see Eq. (6)) for different values of  $E_{su}/Y_{su}$ . The indentation and flattening cases are shown by the solid and dashed lines, respectively. From Fig. 4, we observe that

the value of  $(t/R)_p$  for indentation is almost identical with that for flattening in the range of  $2 \leq P_{c\_co}/P_{c\_su} \leq 9$ . This indicates that the yield inception behavior of an indented coated half space is very similar to that of a flattened coated sphere. In industrial applications, the value of  $P_{c\_co}/P_{c\_su}$  could be beyond the range of  $2 \leq P_{c\_co}/P_{c\_su} \leq 9$ , as for instance, in the case of a carbon overcoat on a magnetic thin film as used in magnetic recording disks (see, e.g., Ref. [36]). Hence, a wide range of  $2 \leq P_{c\_co}/P_{c\_su} \leq 25$  is investigated in this study.

Eq. (7) can be rearranged in the form

$$\left(\frac{t}{R}\right)_p \left(\frac{P_{c\_co}}{P_{c\_su}}\right)^{-0.474} \left(\frac{E_{su}}{Y_{su}}\right)^{1.003} = 2.94 = (\lambda_h)_p \quad (9)$$

where  $\lambda_h$  is defined as a new dimensionless “hard coating parameter” given by

$$\lambda_h = \left(\frac{t}{R}\right) \left(\frac{P_{c\_co}}{P_{c\_su}}\right)^{-0.474} \left(\frac{E_{su}}{Y_{su}}\right)^{1.003} \quad (10)$$

Fig. 5 presents a modified dimensionless critical load in the form  $(P_c/P_{c\_co})/(P_c/P_{c\_co})_{\max}$  as a function of the hard coating parameter  $\lambda_h$  for different values of  $k'$ . As shown in Fig. 5, dividing the original dimensionless critical load  $P_c/P_{c\_co}$  by its peak value  $(P_c/P_{c\_co})_{\max}$ , the curves for different values of  $k'$  were consolidated into a single curve when  $\lambda_h \leq (\lambda_h)_p$ .

Curve fitting of the results presented in Fig. 5 provided a universal expression in the form:

$$\frac{P_c/P_{c\_co}}{(P_c/P_{c\_co})_{\max}} = f_1(\lambda_h, k') = a_1 \lambda_h^{b_1} + c_1 \quad (11)$$

Similar to the behavior of the dimensionless critical load, peak values were also found at the same  $(t/R)_p$  for the dimensionless critical contact area and the dimensionless critical interference. These peak values are:

$$(A_c/A_{c\_co})_{\max} = -1.976 \cdot \kappa^{0.1} + 3.271 \quad (12)$$

$$(\omega_c/\omega_{c\_co})_{\max} = 1.216 \cdot \left(\frac{P_{c\_co}}{P_{c\_su}}\right)^{0.116} \kappa^{-0.297} \quad (13)$$

The following empirical relationships were obtained by curve fitting the numerical simulation results for the modified dimensionless critical contact area  $(A_c/A_{c\_co})/(A_c/A_{c\_co})_{\max}$  and the modified dimensionless critical interference  $(\omega_c/\omega_{c\_co})/(\omega_c/\omega_{c\_co})_{\max}$ :

$$\frac{A_c/A_{c\_co}}{(A_c/A_{c\_co})_{\max}} = f_2(\lambda_h, k') = a_2 \lambda_h^{b_2} + c_2 \quad (14)$$

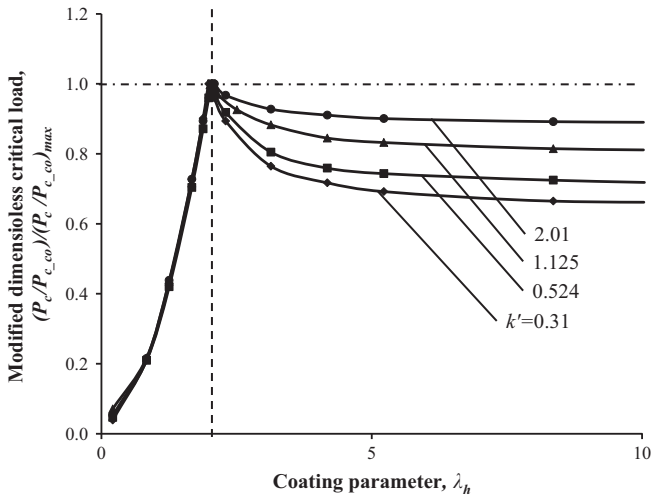


Fig. 5. Modified dimensionless critical load  $(P_c/P_{c\_co})/(P_c/P_{c\_co})_{\max}$  as a function of the coating parameter  $\lambda_h$  for different values of  $k'$ .

$$\frac{\omega_c/\omega_{c\_co}}{(\omega_c/\omega_{c\_co})_{\max}} = f_3(\lambda_h, k') = a_3 \lambda_h^{b_3} + c_3 \quad (15)$$

The coefficients  $a_i$ ,  $b_i$  and  $c_i$  in Eqs. (11), (14) and (15) are summarized in Table 1.

Fig. 6 shows a comparison of the dimensionless critical load  $P_c/P_{c\_co}$  vs. the dimensionless coating thickness  $t/R$  for indentation and flattening. The dimensionless critical load  $P_c/P_{c\_co}$  for indentation and flattening is calculated by the empirical equations derived in this study and the work published in Ref. [35], respectively. The results are shown for  $E_{su}/Y_{su}=952$  and two cases that cover a range of  $P_{c\_co}/P_{c\_su}$  and  $k'$  values: (a)  $P_{c\_co}/P_{c\_su}=8.75$ ,  $k'=0.678$  and (b)  $P_{c\_co}/P_{c\_su}=2$ ,  $k'=0.31$ . From Fig. 6, we observe that the behavior in the cases of indentation (solid lines) and flattening (dashed lines) is very similar. The largest difference between  $P_c/P_{c\_co}$  in indentation and flattening is about 5.1% and 4.2% for cases (a) and (b), respectively.

The results shown in Fig. 6, indicate that in indentation, like in flattening, an optimum coating thickness exists for maximum resistance to plastic yield onset. Also, as was found in Ref. [35], a very small coating thickness can cause weakening of the coated system when  $P_c/P_{c\_co} < (P_{c\_co}/P_{c\_su})^{-1}$ .

Similar to the location of yield inception in the case of a flattened coated sphere described in Ref. [35], the coated substrate indented by a rigid sphere has yield inception in three different locations, shown schematically in Fig. 7. For  $\lambda_h \ll (\lambda_h)_p$  the onset of plastic yield occurs at location 1 within the substrate. For  $\lambda_h < (\lambda_h)_p$  yield inception occurs in location 2, which is in the substrate side of the coating/substrate interface. For  $\lambda_h \geq (\lambda_h)_p$ , the

Table 1  
The coefficients  $a_i$ ,  $b_i$  and  $c_i$  in Eqs. (11), (14) and (15).

i	$\lambda_h \leq (\lambda_h)_p$		
	1	2	3
$a_i$	0.135	0.186	0.2122
$b_i$	1.843	1.43	1.349
$c_i$	0.045	0.161	0.156
i	$\lambda_h > (\lambda_h)_p$		
	1	2	3
$a_i$	$-2.461\kappa^{-0.528} + 4.836$	$-1.892\kappa^{-0.78} + 4.929$	$-1.914\kappa^{-0.52} + 3.561$
$b_i$	-2.24	-2.7	-1.519
$c_i$	$0.7937\kappa^{-0.171}$	$0.25\kappa^{-0.47} + 0.582$	$0.887\kappa^{-0.231} - 0.18$

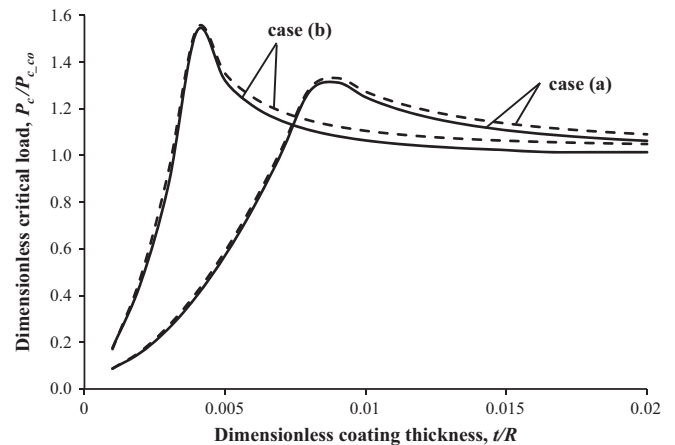


Fig. 6. Dimensionless critical load  $P_c/P_{c\_co}$  vs. dimensionless coating thickness  $t/R$  for indentation (solid lines) and flattening (dashed lines).  $E_{su}/Y_{su}=952$ : (a)  $P_{c\_co}/P_{c\_su}=8.75$ ,  $k'=0.678$  and (b)  $P_{c\_co}/P_{c\_su}=2$ ,  $k'=0.31$ .

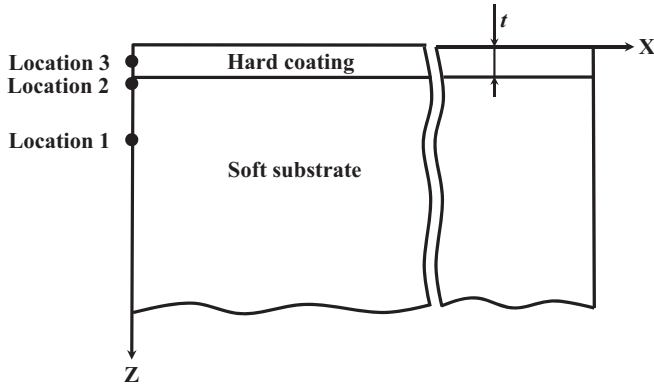


Fig. 7. Schematic description of the three typical locations of yield inception in indentation of a coated substrate.

onset of plastic yield occurs at location 3, which is within the coating.

As an example, consider a rigid sphere with a radius  $R=1$  mm indenting a steel flat with a tungsten coating having the following material properties (see nomenclature below):  $E_{su}=205$  GPa,  $Y_{su}=285$  MPa,  $E_{co}=400$  GPa,  $Y_{co}=750$  MPa, and  $\nu_{su}=\nu_{co}=0.3$ . From Eqs. (3) and (4) one can calculate the critical loads and critical interferences:  $P_{c_{co}}=0.047$  N,  $P_{c_{su}}=0.01$  N,  $\omega_{c_{co}}=18.64$  nm and  $\omega_{c_{su}}=10.25$  nm. Using Eq. (7) the optimum thickness of the coating for best resistance to yield inception is  $t_p=8.4$   $\mu$ m. Using the expression  $\kappa'=(\omega_{c_{co}}/\omega_{c_{su}})/(E_{co}/E_{su})$  we obtain  $\kappa'=0.932$ . Hence, from Eq. (8) the corresponding maximum critical load of the coated system is  $(P_c)_{\max}=0.064$  N and the location of the onset of yield is within the coating (location 3 in Fig. 7).

The critical load  $P_c$  of the coated system is plotted as a function of the coating thickness  $t$  in Fig. 8(a). From this figure we find that for tungsten coating thicknesses  $t$  larger than  $t_p=8.4$   $\mu$ m, the critical load  $P_c$  decreases and eventually approaches the critical load of the tungsten coating  $P_{c_{co}}$ . In this range of coating thicknesses (solid line in Fig. 8(a)) the onset of yield remains within the coating. When  $t$  decreases below  $t_p$  (dashed line in Fig. 8(a)),  $P_c$  decreases as well and the onset of yield moves to the substrate side of the coating–substrate interface (location 2 in Fig. 7). We observe furthermore that for a very thin coating the onset of yielding occurs in the steel substrate (location 1 in Fig. 7). When the coating thickness  $t$  is less than 2.6  $\mu$ m,  $P_c$  becomes smaller than the critical load of the uncoated steel flat  $P_{c_{su}}$ . Hence, at this range of very thin thicknesses the hard tungsten coating is actually causing a weakening effect, which was also noticed by Sun et al. [27] and by Goltsberg et al. [35].

Fig. 8(a) can provide a guideline for a good coating design for this specific coated system indented by a rigid sphere of radius  $R=1$  mm. Tungsten coating thickness  $t$  in the range of  $t < 8.4$   $\mu$ m should be avoided to prevent potential delamination when the onset of plastic deformation is at the coating/substrate interface. The best choice of the tungsten coating thickness is slightly above 8.4  $\mu$ m. In this case the coating provides the maximum protection against yield and also against potential delamination.

Finally, a comparison between the results shown in Fig. 8(a) and a model for an indented coated flat developed by Komvopoulos and Ye [37] is presented in Fig. 8(b). According to the model in [37] the mean contact pressure  $p_m$  and the contact area  $A$  for a coated system in the regime of elastic deformation are given by:

$$p_m = \frac{4\sqrt{2}}{3\pi} \left( \frac{E_e \omega}{Y_e a'} \right) Y_e, A = \frac{1}{2} A' \quad (16)$$

where the truncated contact radius is  $a' = \sqrt{\omega(2R-\omega)}$ , and the truncated contact area is  $A' = \pi(a')^2$ . The equivalent yield strength  $Y_e$

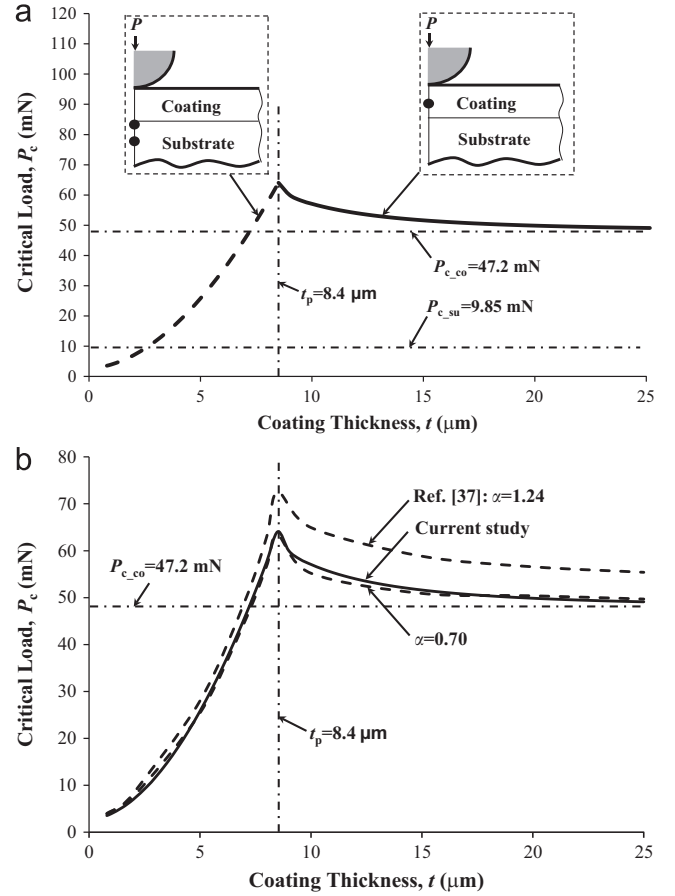


Fig. 8. (a) Critical load,  $P_c$ , as a function of the coating thickness  $t$  for a tungsten coated steel flat system and (b) a comparison with the results based on Ref. [37].

and Young's modulus  $E_e$  of the coated flat indented by a rigid indenter can be calculated from:

$$Y_e = Y_{su} + (Y_{co} - Y_{su}) \exp \left[ - \left( \frac{\omega}{t} \right) \left( \frac{E_{su}}{E_{co}} \right)^{1/2} \right] \quad (17)$$

$$E_e = \left[ (1 - e^{-\alpha t / a \sqrt{\pi}}) \frac{1 - \nu_{co}^2}{E_{co}} + e^{-\alpha t / a \sqrt{\pi}} \frac{1 - \nu_{su}^2}{E_{su}} \right]^{-1} \quad (18)$$

where  $\alpha$  is an empirical parameter depending on the indenter shape [6,7]. Unfortunately, this parameter was not specified in Ref. [37]. To enable a comparison, several values of  $\alpha$  were selected. Substituting the appropriate values for the parameter  $\alpha$ , along with  $\omega = \omega_c$  (obtained from Eqs. (15) and (13)) into Eqs. (16–18), one obtains the critical load  $P_c = (p_m) A_c$  as a function of the coating thickness  $t$ .

The results obtained in the current study and those calculated based on Ref. [37] for tungsten coated steel flat system are shown in Fig. 8(b) (solid and dashed lines). Fair agreement is observed between the current study and Ref. [37] with  $\alpha=1.24$  (see Ref. [7]) for coating thicknesses below  $t_p=8.4$   $\mu$ m. At larger coating thicknesses the critical load based on Ref. [37] with  $\alpha=1.24$  somewhat overestimates the values obtained from the current study. A much better agreement was obtained with  $\alpha=0.7$  for the entire range of coating thickness.

#### 4. Conclusions

A model was developed to investigate the yield inception of a coated half-space indented by a rigid sphere. A universal

dimensionless hard coating parameter  $\lambda_h$  was identified, which controls the critical contact parameters of the indented coated system. Modified dimensionless critical load, critical contact area and critical interference were obtained as functions of a hard coating parameter  $\lambda_h$  and a modified critical interferences ratio  $k'$ .

Three typical different locations of the yield inception of the coated substrate were presented depending on the ratio  $\lambda_h/(\lambda_h)_p$ .

A comparison with previously published results for yield inception of a flattened coated sphere showed that the behavior for both situations is very similar. This is in line with the identical behavior of elastic spherical contact according to the Hertz solution in the absence of any coating.

## References

- [1] Nix WD. Mechanical properties of thin films. *Metallurgical Transactions A* 1989;20(11):2217–45.
- [2] Holmberg K, Matthews A, Ronkainen H. Coatings tribology-contact mechanisms and surface design. *Tribology International* 1998;31(1–3):107–20.
- [3] Holmberg K, Ronkainen H. Tribology of thin coatings. *Ceramics International* 2000;26(7):787–95.
- [4] Mao K, Sun Y, Bloyce A, Bell T. Surface coating effects on contact stress and wear: an approach of surface engineering design and modeling. *Surface Engineering* 2010;26(1–2):142–8.
- [5] Lee S, Yao CD. Microwear mechanism of head carbon film during head disk interface sliding contact. *Tribology International* 2012;45(1):30–7.
- [6] Doerner MF, Nix WD. A method for interpreting the data from depth-sensing indentation instruments. *Journal of Materials Research* 1986;1(4):601–9.
- [7] King RB. Elastic analysis of some punch problems for a layered medium. *International Journal of Solids and Structures* 1987;23(12):1657–64.
- [8] Sun Y, Bell T, Zheng S. Finite element analysis of the critical ratio of coating thickness to indentation depth for coating property measurements by nanoindentation. *Thin Solid Films* 1995;258(1–2):198–204.
- [9] Bhattacharya AK, Nix WD. Analysis of elastic and plastic deformation associated with indentation testing of thin films on substrates. *International Journal of Solids and Structures* 1988;24(12):1287–98.
- [10] Saha R, Nix WD. Effects of the substrate on the determination of thin film mechanical properties by nanoindentation. *Acta Materialia* 2002;50(1):23–38.
- [11] Ye N, Komvopoulos K. Indentation analysis of elastic-plastic homogeneous and layered media: criteria for determining the real material hardness. *ASME Journal of Tribology* 2003;125(4):685–91.
- [12] Antunes JM, Fernandes JV, Sakharova NA, Oliveira MC, Menezes LF. On the determination of the Young's modulus of thin films using indentation tests. *International Journal of Solids and Structures* 2007;44(25–26):8313–34.
- [13] Johnson KL. *Contact Mechanics*. Cambridge: Cambridge University Press; 1985.
- [14] Jaffar MJ. A numerical solution for axisymmetric contact problems involving rigid indenters on elastic layers. *Journal of the Mechanics and Physics of Solids* 1988;36(4):401–16.
- [15] Ramalingam S, Zheng L. Film-substrate interface stresses and their role in the tribological performance of surface coatings. *Tribology International* 1995;28(3):145–61.
- [16] Li J, Chou TW. Elastic field of a thin-film/substrate system under an axisymmetric loading. *International Journal of Solids and Structures* 1997;34(35–36):4463–78.
- [17] Schwarzer N. Arbitrary load distribution on a layered half space. *ASME Journal of Tribology* 2000;122(4):672–81.
- [18] Fretigny C, Chateauminois A. Solution for the elastic field in a layered medium under axisymmetric contact loading. *Journal of Physics D: Applied Physics* 2007;40(18):5418–26.
- [19] Hsuen C-H, Miranda P. Master curves for Hertzian indentation on coating/substrate systems. *Journal of Materials Research* 2004;19(1):94–100.
- [20] Hsuen C-H, Miranda P. Combined empirical-analytical method for determining contact radius and indenter displacement during Hertzian indentation on coating/substrate systems. *Journal of Materials Research* 2004;19(9):2774–81.
- [21] Komvopoulos K. Finite element analysis of a layered elastic solid in normal contact with a rigid surface. *ASME Journal of Tribology* 1988;110(3):477–85.
- [22] Komvopoulos K. Elastic-plastic finite element analysis of indented layered media. *ASME Journal of Tribology* 1989;111(3):430–9.
- [23] Kral ER, Komvopoulos K, Bogy DB. Finite element analysis of repeated indentation of an elastic-plastic layered medium by a rigid sphere, part I: Surface results. *ASME Journal of Applied Mechanics* 1995;62(1):20–8.
- [24] Kral ER, Komvopoulos K, Bogy DB. Finite element analysis of repeated indentation of an elastic-plastic layered medium by a rigid sphere, Part II: Subsurface results. *ASME Journal of Applied Mechanics* 1995;62(1):29–42.
- [25] Sen S, Aksakal B, Ozel A. A finite-element analysis of the indentation of an elastic-work hardening layered half-space by an elastic sphere. *International Journal of Mechanical Sciences* 1998;40(12):1281–93.
- [26] Djabella H, Arnell RD. Finite element analysis of the contact stresses in an elastic coating on an elastic substrate. *Thin Solid Films* 1992;213(2):205–19.
- [27] Sun Y, Bloyce A, Bell T. Finite element analysis of plastic deformation of various TiN coating/substrate systems under normal contact with a rigid sphere. *Thin Solid Films* 1995;271(1–2):122–31.
- [28] Hu X, Lawn B. A simple indentation stress-strain relation for contacts with spheres on bilayer structures. *Thin Solid Films* 1998;322(1–2):232–55.
- [29] Wang JS, Zheng XJ, Zheng H, Zhu Z, Song ST. Evaluation of the substrate effect on indentation behavior of film/substrate system. *Appl Surf Sci* 2010;256(20):5998–6002.
- [30] Kogut L, Etsion I. Elastic-plastic contact analysis of a sphere and a rigid flat. *ASME Journal of Applied Mechanics* 2002;69(5):657–62.
- [31] Jackson RL, Kogut L. A comparison of flattening and indentation approaches for contact mechanics modeling of single asperity contacts. *ASME Journal of Tribology* 2006;128(1):209–12.
- [32] Brizmer V, Kligerman Y, Etsion I. The effect of contact conditions and material properties on the elasticity terminus of a spherical contact. *International Journal of Solids and Structures* 2006;43(18–19):5736–49.
- [33] Li L, Etsion I, Ovcharenko A, Talke FE. The onset of plastic yielding in a spherical shell compressed by a rigid flat. *ASME Journal of Applied Mechanics* 2011;78(1):011016.
- [34] Li L, Wang L, Etsion I, Talke FE. The effect of contact conditions and material properties on plastic yield inception in a spherical shell compressed by a rigid flat. *International Journal of Solids and Structures* 2011;48(3–4):463–71.
- [35] Goltsberg R, Etsion I, Davidi G. The onset of plastic yielding in a coated sphere compressed by a rigid flat. *Wear* 2011;271(11–12):2968–77.
- [36] Komvopoulos K. Head-disk interface contact mechanics for ultrahigh density magnetic recording. *Wear* 2000;238(1):1–11.
- [37] Komvopoulos K, Ye N. Three-dimensional contact analysis of elastic-plastic layered media with fractal surface topographies. *ASME Journal of Tribology* 2001;123(3):632–40.